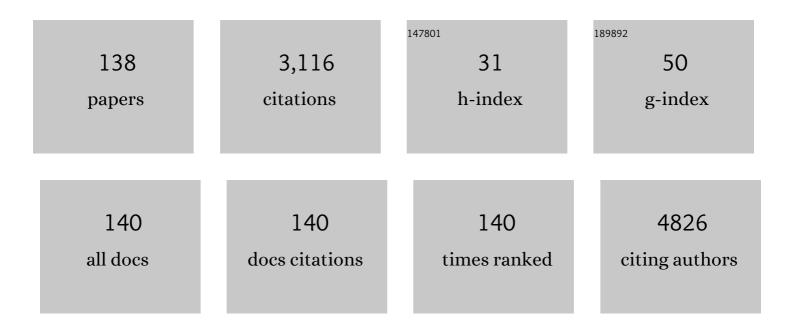
List of Publications by Year in descending order

Source: https://exaly.com/author-pdf/774941/publications.pdf Version: 2024-02-01



#	Article	IF	CITATIONS
1	A Lamellar Yolk–Shell Lithiumâ€&ulfur Battery Cathode Displaying Ultralong Cycling Life, High Rate Performance, and Temperature Tolerance. Advanced Science, 2022, 9, e2103517.	11.2	20
2	A novel free-standing metal organic frameworks-derived cobalt sulfide polyhedron array for shuttle effect suppressive lithium–sulfur batteries. Nanotechnology, 2022, 33, 105401.	2.6	2
3	Encapsulating Metal-Organic-Framework Derived Nanocages into a Microcapsule for Shuttle Effect-Suppressive Lithium-Sulfur Batteries. Nanomaterials, 2022, 12, 236.	4.1	5
4	A novel "caterpillar with eggs―mesostructured iron sulfide as an anode for a Li-ion battery displaying stable electrochemical performance. Chemical Communications, 2022, 58, 1561-1564.	4.1	7
5	BiOCl Nanorings with Co-Exposed (110)/(001) Facets for Photocatalytic Degradation of Organic Dyes. ACS Applied Nano Materials, 2022, 5, 2476-2482.	5.0	12
6	Engineering a ternary one-dimensional Fe ₂ P@SnP _{0.94} @MoS ₂ mesostructure through magnetic-field-induced self-assembly as a high-performance lithium-ion battery anode. Chemical Communications, 2022, 58, 5108-5111.	4.1	5
7	A graphene oxide scaffold-encapsulated microcapsule for polysulfide-immobilized long life lithium–sulfur batteries. Lab on A Chip, 2022, 22, 2185-2191.	6.0	5
8	Self-assembly of magnetic nanoparticles as one-dimensional sulfur host for stable lithium-sulfur batteries. Journal of Electroanalytical Chemistry, 2022, 916, 116371.	3.8	0
9	A lamellar V ₂ 0 ₃ @C composite for aluminium-ion batteries displaying long cycle life and low-temperature tolerance. Chemical Communications, 2022, 58, 7172-7175.	4.1	9
10	A flexible self-healing Zn ₃ V ₂ O ₇ (OH) ₂ ·2H ₂ O-based Zn-ion battery under continuous folding and twisting. Chemical Communications, 2022, 58, 8117-8120.	4.1	7
11	Ultra-fast and accurate binding energy prediction of shuttle effect-suppressive sulfur hosts for lithium-sulfur batteries using machine learning. Energy Storage Materials, 2021, 35, 88-98.	18.0	42
12	General Liquidâ€Driven Coaxial Flow Focusing Preparation of Novel Microcapsules for Rechargeable Magnesium Batteries. Advanced Science, 2021, 8, 2002298.	11.2	20
13	Self-reduction preparation of porous multi-walled ZnCo2O4 spheres as sulfur host for lithium‑sulfur battery cathodes with long cycling life and stable rate-performance. Journal of Electroanalytical Chemistry, 2021, 880, 114860.	3.8	6
14	A General Templateâ€Induced Sulfuration Approach for Preparing Bifunctional Hollow Sulfides for Highâ€Performance Al―and Liâ€ion Batteries. Energy Technology, 2021, 9, 2000900.	3.8	5
15	A coaxial spiral SiO2@Fe2O3 nanowire as lithium-ion battery anode exhibiting stable rate-performance. Materials Letters, 2021, 285, 129107.	2.6	10
16	A rod-on-tube CoMoO4@hydrogel composite as lithium-ion battery anode with high capacity and stable rate-performance. Journal of Alloys and Compounds, 2021, 858, 157648.	5.5	14
17	A novel rose-with-thorn ternary MoS ₂ @carbon@polyaniline nanocomposite as a rechargeable magnesium battery cathode displaying stable capacity and low-temperature performance. Nanoscale Advances, 2021, 3, 5576-5580.	4.6	13
18	A yolk–shell Fe ₃ O ₄ @void@carbon nanochain as shuttle effect suppressive and volume-change accommodating sulfur host for long-life lithium–sulfur batteries. Nanoscale, 2021, 13, 7744-7750.	5.6	19

#	Article	IF	CITATIONS
19	A Selfâ€Healing Flexible Quasiâ€Solid Zincâ€Ion Battery Using Allâ€Inâ€One Electrodes. Advanced Science, 2021 2004689.	, 8, 11.2	54
20	Ab initio determination of crystal stability of di-p-tolyl disulfide. Scientific Reports, 2021, 11, 7076.	3.3	4
21	Electron and Ion Transport of Tin Dioxide in Secondary Batteries: Enhancement Approaches, Mechanisms, and Performance. Frontiers in Physics, 2021, 9, .	2.1	1
22	Machine learning builds full-QM precision protein force fields in seconds. Briefings in Bioinformatics, 2021, 22, .	6.5	8
23	A Self-Healing Lithium–Sulfur Battery Using Gel-Infilled Microcapsules. ACS Applied Energy Materials, 2021, 4, 6749-6756.	5.1	10
24	Engineering Nanostructured Silicon and its Practical Applications in Lithiumâ€Ion Batteries: A Critical Review. Energy Technology, 2021, 9, 2100400.	3.8	9
25	A matryoshka-like CuS@void@Co3O4 double microcube-locked sulfur as cathode for high-performance lithium-sulfur batteries. Ceramics International, 2021, 47, 25769-25776.	4.8	5
26	Engineering nanocluster arrays on lotus leaf as free-standing high areal capacity Li-ion battery anodes: A cost-effective and general bio-inspired approach. Journal of Alloys and Compounds, 2021, , 162136.	5.5	2
27	A Polysulfidesâ€Confined Allâ€inâ€One Porous Microcapsule Lithium–Sulfur Battery Cathode. Small, 2021, 17, e2103051.	10.0	21
28	A Microcapsuleâ€Assistant Selfâ€Healing Magnesium Battery Cathodes. Energy Technology, 2021, 9, 2100393.	3.8	2
29	A binder-free lithium-sulfur battery cathode using three-dimensional porous g-C3N4 nanoflakes as sulfur host displaying high binding energies with lithium polysulfides. Journal of Alloys and Compounds, 2021, 881, 160629.	5.5	12
30	A novel nanosheets-coated multi-layered SnO2@NiMoO4 microsphere as high-performance Li-ion battery anode. Journal of Alloys and Compounds, 2021, 889, 161733.	5.5	4
31	Predicting adsorption ability of adsorbents at arbitrary sites for pollutants using deep transfer learning. Npj Computational Materials, 2021, 7, .	8.7	22
32	A novel nanosphere-in-nanotube iron phosphide Li-ion battery anode displaying a long cycle life, recoverable rate-performance, and temperature tolerance. Nanoscale, 2021, 13, 15624-15630.	5.6	8
33	An encapsulation–reduction–catalysis confined all-in-one microcapsule for lithium–sulfur batteries displaying a high capacity and stable temperature tolerance. Materials Chemistry Frontiers, 2021, 5, 4565-4570.	5.9	6
34	Novel Doughnutlike Graphene Quantum Dot-Decorated Composites for High-Performance Li–S Batteries Displaying Dual Immobilization Toward Polysulfides. ACS Applied Energy Materials, 2021, 4, 10998-11003.	5.1	7
35	Quantum Mechanical-Based Stability Evaluation of Crystal Structures for HIV-Targeted Drug Cabotegravir. Molecules, 2021, 26, 7178.	3.8	1
36	Engineering a novel microcapsule of Cu9S5 core and SnS2 quantum dot/carbon nanotube shell as a Li-ion battery anode. Chemical Communications, 2021, 57, 13397-13400.	4.1	4

#	Article	IF	CITATIONS
37	Electrodeposition Technologies for Liâ€Based Batteries: New Frontiers of Energy Storage. Advanced Materials, 2020, 32, e1903808.	21.0	70
38	A novel spring-structured coaxial hierarchical SiO ₂ @Co ₃ O ₄ nanowire as a lithium-ion battery anode and its <i>in situ</i> real-time lithiation. Nanotechnology, 2020, 31, 035401.	2.6	8
39	A novel binary metal sulfide hybrid Li-ion battery anode: Three-dimensional ZnCo2S4/NiCo2S4 derived from metal-organic foams enables an improved electron transfer and ion diffusion performance. Journal of Alloys and Compounds, 2020, 817, 153293.	5.5	24
40	An artificial sea urchin with hollow spines: improved mechanical and electrochemical stability in high-capacity Li–Ge batteries. Nanoscale, 2020, 12, 5812-5816.	5.6	4
41	Engineering early prediction of supercapacitors' cycle life using neural networks. Materials Today Energy, 2020, 18, 100537.	4.7	14
42	A metal organic foam-derived multi-layered and porous copper sulfide scaffold as sulfur host with multiple shields for preventing shuttle effect in lithium-sulfur batteries. Electrochimica Acta, 2020, 356, 136853.	5.2	17
43	Molecular structure determination of solid carbon dioxide phase IV at high pressures and temperatures based on MÃ,llerâ€Plesset perturbation theory. International Journal of Quantum Chemistry, 2020, 120, e26397.	2.0	9
44	A novel ultrathin single-crystalline Bi2O3 nanosheet wrapped by reduced graphene oxide with improved electron transfer for Li storage. Journal of Solid State Electrochemistry, 2020, 24, 2487-2497.	2.5	8
45	Polymer Composites Containing Phaseâ€Change Microcapsules Displaying Deep Undercooling Exhibit Thermal Historyâ€Dependent Mechanical Properties. Advanced Materials Technologies, 2020, 5, 2000286.	5.8	14
46	Microcapsules: Polymer Composites Containing Phaseâ€Change Microcapsules Displaying Deep Undercooling Exhibit Thermal Historyâ€Dependent Mechanical Properties (Adv. Mater. Technol. 10/2020). Advanced Materials Technologies, 2020, 5, 2070062.	5.8	1
47	Ab initio phase transition prediction for ices XV/XIV/VIII at high pressures and low temperatures. Chemical Physics Letters, 2020, 760, 138015.	2.6	3
48	Encapsulating Tin Nanoflowers into Microcapsules for Highâ€Rateâ€Performance Secondary Battery Anodes through In Situ Polymerizing Oilâ€inâ€Water Interface. Energy Technology, 2020, 8, 2070055.	3.8	0
49	Ab Initio Prediction of the Phase Transition for Solid Ammonia at High Pressures. Scientific Reports, 2020, 10, 7546.	3.3	5
50	Silicon Quantum Dots Induce Uniform Lithium Plating in a Sandwiched Metal Anode. ChemElectroChem, 2020, 7, 2026-2032.	3.4	8
51	A metal organic foam-derived zinc cobalt sulfide with improved binding energies towards polysulfides for lithium–sulfur batteries. Ceramics International, 2020, 46, 14056-14063.	4.8	22
52	Hydrogel and sulfur co-coating on semispherical TiO2 as polysulfides-immobilized cathodes for high capacity and stable rate performance lithium-sulfur batteries. Applied Surface Science, 2020, 513, 145887.	6.1	25
53	Encapsulating Tin Nanoflowers into Microcapsules for Highâ€Rateâ€Performance Secondary Battery Anodes through In Situ Polymerizing Oilâ€inâ€Water Interface. Energy Technology, 2020, 8, 1901404.	3.8	2
54	An oriented laterally-growing NiCo ₂ O ₄ nanowire array on a Fe ₂ O ₃ microdisc as a high-capacity and excellent rate-performance secondary battery anode. Chemical Communications, 2020, 56, 2618-2621.	4.1	11

#	Article	IF	CITATIONS
55	A Novel Mechanically Robust Leafâ€Shaped Tin Dioxide Liâ€Ion Battery Anode and Its Dynamic Structural Transformation and Electronâ€Transfer Simulation. Energy Technology, 2020, 8, 1901149.	3.8	1
56	Phase Transition of Ice at High Pressures and Low Temperatures. Molecules, 2020, 25, 486.	3.8	3
57	Environmentally Friendly and Cost-Effective Synthesis of Carbonaceous Particles for Preparing Hollow SnO2 Nanospheres and their Bifunctional Li-Storage and Gas-Sensing Properties. Crystals, 2020, 10, 231.	2.2	4
58	A novel silicon nanoparticles-infilled capsule prepared by an oil-in-water emulsion strategy for high-performance Li-ion battery anodes. Nanotechnology, 2020, 31, 335403.	2.6	6
59	A novel sulfur@void@hydrogel yolk-shell particle with a high sulfur content for volume-accommodable and polysulfide-adsorptive lithium-sulfur battery cathodes. Nanotechnology, 2020, 31, 455402.	2.6	8
60	A cataluminescence sensor for the detection of trichloroethylene based on PEG200/ZnO nanocomposite. E3S Web of Conferences, 2020, 212, 02004.	0.5	0
61	Peonyâ€like Na ₂ Mg(CO ₃) ₂ : a nanomaterial with the characteristic of high sensitivity and rapid response for the detection of alcohols. Micro and Nano Letters, 2020, 15, 915-919.	1.3	0
62	A Bioâ€Inspired Structurallyâ€Responsive and Polysulfidesâ€Mobilizable Carbon/Sulfur Composite as Longâ€Cycling Life Liâ^'S Battery Cathode. ChemElectroChem, 2019, 6, 3966-3975.	3.4	13
63	Synthesis of Uniform Alkane-Filled Capsules with a High Under-Cooling Performance and Their Real-Time Optical Properties. Polymers, 2019, 11, 199.	4.5	0
64	A helix-shaped polyaniline/sulfur nanowire as novel structure-accommodable lithium-sulfur battery cathode for high-performance electrochemical lithium-storage. Journal of Electroanalytical Chemistry, 2019, 855, 113543.	3.8	8
65	Low-Temperature Polymorphic Transformation of \hat{I}^2 -Lactam Antibiotics. Crystals, 2019, 9, 460.	2.2	4
66	An all-in-one Sn–Co alloy as a binder-free anode for high-capacity batteries and its dynamic lithiation in situ. Chemical Communications, 2019, 55, 529-532.	4.1	9
67	Crystal Structure Optimization and Gibbs Free Energy Comparison of Five Sulfathiazole Polymorphs by the Embedded Fragment QM Method at the DFT Level. Crystals, 2019, 9, 256.	2.2	7
68	A nickel oxide nanoflakes/reduced graphene oxide composite and its high-performance lithium-storage properties. Journal of Solid State Electrochemistry, 2019, 23, 2173-2180.	2.5	7
69	High-performance ternary nickel-cobalt-manganese oxide nanoparticles-anchored reduced graphene oxide composite as Li-ion battery cathode: Simple preparation and comparative study. Ceramics International, 2019, 45, 20105-20112.	4.8	2
70	A novel ternary sulfur/carbon@tin dioxide composite with polysulfides-adsorptive shell and conductive core as high-performance lithium‑sulfur battery cathodes. Applied Surface Science, 2019, 489, 462-469.	6.1	16
71	A hollow Co2SiO4 nanosheet Li-ion battery anode with high electrochemical performance and its dynamic lithiation/delithiation using in situ transmission electron microscopy technology. Applied Surface Science, 2019, 490, 510-515.	6.1	14
72	Preparation of reduced graphene oxide@nickel oxide nanosheets composites with enhanced lithium-ion storage performance. Materials Chemistry and Physics, 2019, 232, 229-239.	4.0	6

#	Article	IF	CITATIONS
73	Three-Dimensionally Porous Li-Ion and Li-S Battery Cathodes: A Mini Review for Preparation Methods and Energy-Storage Performance. Nanomaterials, 2019, 9, 441.	4.1	12
74	(Co/Fe) ₄ O ₄ Cubane-Containing Nanorings Fabricated by Phosphorylating Cobalt Ferrite for Highly Efficient Oxygen Evolution Reaction. ACS Catalysis, 2019, 9, 3878-3887.	11.2	38
75	A hydrogel-coated porous sulfur particle as volume-accommodable, conductivity-improved, and polysulfide-adsorptive cathode for lithium‑sulfur batteries. Journal of Electroanalytical Chemistry, 2019, 841, 26-35.	3.8	11
76	Threeâ€Dimensionally Scaffolded Hydrogel@Sulfur Composite as a Binderâ€Free Polysulfidesâ€Adsorptive Cathode for Highâ€Performance Lithiumâ€6ulfur Batteries. Energy Technology, 2019, 7, 1801158.	3.8	3
77	A bee pupa-infilled honeycomb structure-inspired Li ₂ MnSiO ₄ cathode for high volumetric energy density secondary batteries. Chemical Communications, 2019, 55, 3582-3585.	4.1	4
78	High capacity 3D structured tin-based electroplated Li-ion battery anodes. Energy Storage Materials, 2019, 17, 151-156.	18.0	36
79	A novel biomimetic dandelion structure-inspired carbon nanotube coating with sulfur as a lithium–sulfur battery cathode. Nanotechnology, 2019, 30, 155401.	2.6	16
80	A novel wheel-confined composite as cathode in Li-S batteries with high capacity retention. Journal of Alloys and Compounds, 2019, 776, 504-510.	5.5	11
81	A biomimetic SiO2@chitosan composite as highly-efficient adsorbent for removing heavy metal ions in drinking water. Chemosphere, 2019, 214, 738-742.	8.2	64
82	Ni-encapsulated TiO2 nanotube array prepared using atomic layer deposition as a high-performance Li-ion battery anode. Materials Letters, 2018, 219, 12-15.	2.6	10
83	Hydrogel assisted synthesis of Li3V2(PO4)3 composite as high energy density and low-temperature stable secondary battery cathode. Journal of Alloys and Compounds, 2018, 739, 837-847.	5.5	10
84	Three-dimensional sandwich-structured NiMn2O4@reduced graphene oxide nanocomposites for highly reversible Li-ion battery anodes. Journal of Power Sources, 2018, 378, 677-684.	7.8	47
85	A high-capacity NiCo2O4@reduced graphene oxide nanocomposite Li-ion battery anode. Journal of Alloys and Compounds, 2018, 741, 223-230.	5.5	41
86	General approach for preparing sandwich-structured metal sulfide@reduced graphene oxide as highly reversible Li-ion battery anode. Materials Research Letters, 2018, 6, 307-313.	8.7	12
87	High Electrochemical Sensitivity of TiO _{2–<i>x</i>} Nanosheets and an Electron-Induced Mutual Interference Effect toward Heavy Metal Ions Demonstrated Using X-ray Absorption Fine Structure Spectra. Analytical Chemistry, 2018, 90, 4328-4337.	6.5	52
88	Low Interface Energies Tune the Electrochemical Reversibility of Tin Oxide Composite Nanoframes as Lithium-Ion Battery Anodes. ACS Applied Materials & Interfaces, 2018, 10, 36892-36901.	8.0	19
89	Highly sensitive and selective butanol sensors using the intermediate state nanocomposites converted from β-FeOOH to α-Fe2O3. Sensors and Actuators B: Chemical, 2018, 273, 543-551.	7.8	58
90	A novel litchi-like LiFePO4 sphere/reduced graphene oxide composite Li-ion battery cathode with high capacity, good rate-performance and low-temperature property. Applied Surface Science, 2018, 459, 233-241.	6.1	30

#	Article	IF	CITATIONS
91	Interlayer Lithium Plating in Au Nanoparticles Pillared Reduced Graphene Oxide for Lithium Metal Anodes. Advanced Functional Materials, 2018, 28, 1804133.	14.9	142
92	Surface-Electronic-State-Modulated, Single-Crystalline (001) TiO ₂ Nanosheets for Sensitive Electrochemical Sensing of Heavy-Metal Ions. Analytical Chemistry, 2017, 89, 3386-3394.	6.5	104
93	Three-dimensional graphene-based nanocomposites for high energy density Li-ion batteries. Journal of Materials Chemistry A, 2017, 5, 5977-5994.	10.3	67
94	Electroplating lithium transition metal oxides. Science Advances, 2017, 3, e1602427.	10.3	62
95	In situ gold nanoparticle-decorated three-dimensional tin dioxide nanostructures for sensitive and selective gas-sensing detection of volatile organic compounds. Journal of Materials Chemistry C, 2017, 5, 6193-6201.	5.5	13
96	Facile synthesis of chitosan nanoparticle-modified MnO2 nanoflakes for ultrafast adsorption of Pb(II) from aqueous solution. Water Science and Technology: Water Supply, 2017, 17, 32-38.	2.1	7
97	Improved Performance in FeF ₂ Conversion Cathodes through Use of a Conductive 3D Scaffold and Al ₂ O ₃ ALD Coating. Advanced Functional Materials, 2017, 27, 1702783.	14.9	55
98	A novel tin hybrid nano-composite with double nets of carbon matrixes as a stable anode in lithium ion batteries. Chemical Communications, 2017, 53, 13125-13128.	4.1	7
99	Catalysis-Based Cataluminescent and Conductometric Gas Sensors: Sensing Nanomaterials, Mechanism, Applications and Perspectives. Catalysts, 2016, 6, 210.	3.5	8
100	Heteroepitaxial Growth of GaN on Unconventional Templates and Layerâ€Transfer Techniques for Largeâ€Area, Flexible/Stretchable Lightâ€Emitting Diodes. Advanced Optical Materials, 2016, 4, 505-521.	7.3	27
101	Three-dimensional MgSiO3-coated SnO2/C nanostructures for efficient adsorption of heavy metal ions from aqueous solution. RSC Advances, 2016, 6, 73412-73420.	3.6	4
102	Lithiumâ€lon Batteries: Graphene Sandwiched Mesostructured Liâ€lon Battery Electrodes (Adv. Mater.) Tj ETQqC	0 0 rgBT 21.0	/Oyerlock 10
103	Graphene Sandwiched Mesostructured Liâ€lon Battery Electrodes. Advanced Materials, 2016, 28, 7696-7702.	21.0	86
104	High Volumetric Capacity Three-Dimensionally Sphere-Caged Secondary Battery Anodes. Nano Letters, 2016, 16, 4501-4507.	9.1	62
105	Integration of high capacity materials into interdigitated mesostructured electrodes for high energy and high power density primary microbatteries. Journal of Power Sources, 2016, 315, 308-315.	7.8	32
106	Photonic Crystals: Template-Directed Directionally Solidified 3D Mesostructured AgCl-KCl Eutectic Photonic Crystals (Adv. Mater. 31/2015). Advanced Materials, 2015, 27, 4550-4550.	21.0	0
107	High Fullâ€Electrode Basis Capacity Templateâ€Free 3D Nanocomposite Secondary Battery Anodes. Small, 2015, 11, 6265-6271.	10.0	14
108	Templateâ€Directed Directionally Solidified 3D Mesostructured AgCl–KCl Eutectic Photonic Crystals. Advanced Materials, 2015, 27, 4551-4559.	21.0	28

#	Article	IF	CITATIONS
109	Mechanically and Chemically Robust Sandwich-Structured C@Si@C Nanotube Array Li-Ion Battery Anodes. ACS Nano, 2015, 9, 1985-1994.	14.6	119
110	Three-dimensionally scaffolded Co3O4 nanosheet anodes with high rate performance. Journal of Power Sources, 2015, 299, 40-48.	7.8	21
111	Biomimetic snowflake-shaped magnetic micro-/nanostructures for highly efficient adsorption of heavy metal ions and organic pollutants from aqueous solution. Journal of Materials Chemistry A, 2014, 2, 11759-11767.	10.3	34
112	Hydrothermal Fabrication of Threeâ€Dimensional Secondary Battery Anodes. Advanced Materials, 2014, 26, 7096-7101.	21.0	48
113	A three-dimensional hierarchical CdO nanostructure: Preparation and its improved gas-diffusing performance in gas sensor. Sensors and Actuators B: Chemical, 2013, 184, 260-267.	7.8	33
114	Modification of coral-like SnO2 nanostructures with dense TiO2 nanoparticles for a self-cleaning gas sensor. Talanta, 2012, 99, 394-403.	5.5	15
115	Novel hierarchically-packed tin dioxide sheets for fast adsorption of organic pollutant in aqueous solution. Journal of Materials Chemistry, 2012, 22, 2885-2893.	6.7	13
116	Preparation of a leaf-like CdS micro-/nanostructure and its enhanced gas-sensing properties for detecting volatile organic compounds. Journal of Materials Chemistry, 2012, 22, 17782.	6.7	82
117	Sensitive detection of indoor air contaminants using a novel gas sensor based on coral-shaped tin dioxide nanostructures. Sensors and Actuators B: Chemical, 2012, 165, 24-33.	7.8	8
118	Dense doping of indium to coral-like SnO ₂ nanostructures through a plasma-assisted strategy for sensitive and selective detection of chlorobenzene. Nanotechnology, 2011, 22, 315501.	2.6	21
119	Detection of heroin covered by skin by using robust principal components analysis. Measurement: Journal of the International Measurement Confederation, 2011, 44, 267-273.	5.0	8
120	Differences of element distribution between free and wheel side surface of NdFeB/α-Fe ribbons. Journal of Rare Earths, 2011, 29, 94-96.	4.8	2
121	A novel porous anodic alumina based capacitive sensor towards trace detection of PCBs. Sensors and Actuators B: Chemical, 2011, 157, 641-646.	7.8	21
122	Synthesis of novel layer-packed In <inf>2</inf> O <inf>3</inf> nanostructures and their application in gas sensor for detecting indoor air contaminants. , 2011, , .		0
123	Novel nanoparticle detection method using electrochemical device based on anodic aluminum oxide nanopore membrane. Procedia Engineering, 2010, 7, 100-105.	1.2	1
124	Comparison on gas-sensing properties of single- and multi-layered SnO2 nanostructures in drug-precursors detection. Procedia Engineering, 2010, 7, 123-129.	1.2	1
125	Mesoporous SnO2 sensor prepared by carbon nanotubes as template and its sensing properties to indoor air pollutants. Procedia Engineering, 2010, 7, 172-178.	1.2	13
126	A novel coral-like porous SnO ₂ hollow architecture: biomimetic swallowing growth mechanism and enhanced photovoltaic property for dye-sensitized solar cell application. Chemical Communications, 2010, 46, 472-474.	4.1	120

#	Article	IF	CITATIONS
127	Novel facile detection of persistent organic pollutants using highly sensitive gas sensor. Talanta, 2010, 82, 409-416.	5.5	5
128	Porous Hierarchical In ₂ O ₃ Micro-/Nanostructures: Preparation, Formation Mechanism, and Their Application in Gas Sensors for Noxious Volatile Organic Compound Detection. Journal of Physical Chemistry C, 2010, 114, 4887-4894.	3.1	111
129	A novel ammonia sensor based on high density, small diameter polypyrrole nanowire arrays. Sensors and Actuators B: Chemical, 2009, 142, 204-209.	7.8	80
130	Shape- and phase-controlled synthesis of In2O3 with various morphologies and their gas-sensing properties. Sensors and Actuators B: Chemical, 2009, 137, 103-110.	7.8	94
131	Triethylenetetramine (TETA)-assisted synthesis, dynamic growth mechanism, and photoluminescence properties of radial single-crystalline ZnS nanowire bundles. Journal of Crystal Growth, 2009, 311, 1423-1429.	1.5	21
132	Synthesis of close-packed multi-walled carbon nanotube bundles using Mo as catalyst. Carbon, 2009, 47, 1652-1658.	10.3	31
133	In Situ Growth of Tin Oxide Nanowires, Nanobelts, and Nanodendrites On the Surface of Iron-Doped Tin Oxide/Multiwalled Carbon Nanotube Nanocomposites. Journal of Physical Chemistry C, 2009, 113, 20583-20588.	3.1	9
134	Nanomaterial-Assisted Signal Enhancement of Hybridization for DNA Biosensors: A Review. Sensors, 2009, 9, 7343-7364.	3.8	43
135	Novel Single-Crystalline Hierarchical Structured ZnO Nanorods Fabricated via a Wet-Chemical Route: Combined High Gas Sensing Performance with Enhanced Optical Properties. Crystal Growth and Design, 2009, 9, 1716-1722.	3.0	67
136	Template synthesis, organic gas-sensing and optical properties of hollow and porous In ₂ O ₃ nanospheres. Nanotechnology, 2008, 19, 345704.	2.6	106
137	A Novel Antimonyâ^'Carbon Nanotubeâ^'Tin Oxide Thin Film:  Carbon Nanotubes as Growth Guider and Energy Buffer. Application for Indoor Air Pollutants Gas Sensor. Journal of Physical Chemistry C, 2008, 112, 6119-6125.	3.1	54
138	Flower-shaped nanoscale Na2Mg(CO3)2: a promising adsorbent for fluoride removal from drinking water. , 0, 202, 232-240.		2